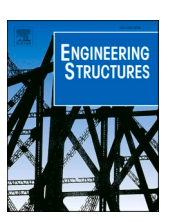
ELSEVIER

Contents lists available at ScienceDirect

Engineering Structures

journal homepage: www.elsevier.com/locate/engstruct





Towards seismic performance quantification of viscous damped steel structure: Site-specific hazard analysis and response prediction

Baiping Dong a,*, James M. Ricles b

- ^a College of Civil Engineering, Tongji University, Shanghai 200092, PR China
- ^b Department of Civil and Environmental Engineering, Lehigh University, Bethlehem, PA 18015, USA

ARTICLE INFO

Keywords: Damping system Earthquake resilience Site-specific hazard analysis Ground motion selection Response quantification

ABSTRACT

With an emphasis on predictable performance, the paramount importance of performance-based earthquake engineering (PBEE) in quantifying earthquake risks and facilitating the better-informed design of the built environment to achieve earthquake resilience has been widely acknowledged. And the uses of damping systems, i.e., structures incorporated with supplemental damping devices, have been recognized as an effective structural development to increase the resilience of structures to earthquakes. This paper presents a uniform hazard spectrum (UHS) based site-specific ground motion selection procedure, to implement the PBEE framework to relate earthquake hazard to structural performance for structures with variable dynamic properties. This ground motion selection procedure accounts for the effect of variable structural dynamic properties on hazard characterization for structures with damping systems. A paradigm building site, on which the site-specific hazard from the probabilistic seismic hazard analysis (PSHA) is consistent with the risk-targeted hazard from the design maps of ASCE/SEI 7-10, is selected for the implementation of the procedure. Three suites of 40 ground motions representing various hazard intensities at the building site are selected for time history dynamic analysis of a prototype structure with nonlinear viscous damping system. Evaluated is the probability distribution of major engineering demand parameters (EDPs) including story drift, residual story drift, floor velocity, and floor acceleration. The results demonstrated that the major EDPs of a building structure with supplemental nonlinear viscous dampers at a paradigm site can be estimated using the lognormal probability distribution, and the proposed UHS-based site-specific ground motion selection procedure is critical to the performance assessment of structures with variable dynamic properties in the PBEE framework.

1. Introduction

The idea of earthquake resilience has been zealously endorsed over the past two decades when disastrous earthquake events in very different parts of the world have questioned the capability of communities to reduce casualties, structural damages, and interruptions of infrastructural facilities, when they are stroked by these extreme events. In this regard, the need to establish earthquake-resilient communities has been identified as the frontier challenge to be addressed by earthquake engineering research in a substantial amount of published works on earthquake resilience [1–8]. As outlined in these published works, a key aspect of resilience is to mitigate the lasting effects of earthquakes on society and enhance the capacity for disaster recovery. Focused on the question of how to increase the post-earthquake operationally of structures and infrastructure facilities that are critical to a community's

needs in the aftermath of a major earthquake, researchers (e.g., Burton et al. [9] and Bruneau et al. [10]) have discussed the engineering aspects of resilient communities and identified the engineering challenges on the way to the built of resilient communities. One of the greatest challenges is to introduce resilience measure metrics and quantify resilience for evaluation, which demands for methods to determine the expected response of structures and to relate this to meaningful performance metrics. With an emphasis on providing predictable performance under multiple levels of earthquakes, the role of performance-based earthquake engineering (PBEE) [11–12] in quantifying earthquake risks and facilitating the better-informed design of the built environment has been regarded of paramount important to the establishment of earthquake resilient communities. To address specific aspects of resilience, major developments have been accomplished in PBEE over the past two decades to relate quantitative measures of earthquake hazard to system

E-mail address: baipingdong@tongji.edu.cn (B. Dong).

^{*} Corresponding author.

performance metrics through probabilistic seismic hazard analysis (PSHA) [13–14], advanced modeling and nonlinear response history analysis [15–16], and performance quantification and assessment [17–18]. As a result, performance quantification in terms of direct economic losses and collapse risk due to earthquakes, as well as other performance measures including risks of building closure, repair times, and casualties are all included in the latest generation of PBEE framework [12].

As one of the critical components of the PBEE framework for risk assessment, the purpose of seismic hazard analysis is to characterize earthquake hazard in terms of a ground motion intensity measure and select ground motions to represent the characterized hazard for the site of interest. Conventionally, the 5-percent damped spectral acceleration for a given earthquake event at the fundamental period of a structure is used to represent the ground motion intensity measure [19]. And, the uniform hazard spectrum (UHS) from PSHA, of which the spectral accelerations at each period have a uniform probability of exceedance (POE) (e.g., 10% POE in 50 years), has been widely adopted as the target hazard spectrum for ground motion selection. In the meantime, alternative hazard intensity measures and target hazard spectrum that are supposed to be more suitable than the UHS have been put forward by researchers for ground motion selection for better structural response quantification [20-26]. Particularly, Baker and Cornell [20-21] proposed the vector-valued intensity measure consisting of spectral acceleration and spectral shape indicator to account for the effect of ground motion spectral shape on structural response. Based on this, the conditional mean spectrum (CMS), of which the spectral accelerations were computed conditional on a target spectral acceleration at a single period, was proposed to be used as a target spectrum for ground motion selection [22]. As the CMS accounts for the correlation in spectral accelerations at multiple periods, it has been regarded maintains the probabilistic rigor of PSHA, and therefore, can be utilized as a useful target spectrum to select ground motions to enable better quantitative assessments about the probability distribution of structural response from dynamic analysis. Accordingly, as an alternative to conventional ground motion selection approaches utilizing the UHS as the target hazard spectrum, this CMS-based ground motion selection approach has gained increasing popularity in probabilistic seismic engineering assessments. As a result, institutional reports such as the PEER report 2009/01 [27] and the NIST [28] have included both the UHS and CMSbased approaches for ground motion selection for code-based design and performance assessment of buildings using time history dynamic analvsis. Nevertheless, as the CMS conditions on the spectral acceleration at a single period, challenges remain for implementing this CMS-based ground motion selection approach for structures sensitive to excitation at multiple periods and accurate quantification of variability in response. Moreover, with the ongoing development of structural systems that are sensitive to loading rate for earthquake-resilient design, it is of great importance to identify the most suitable ground motion selection approach that benefits probability observation of structural response and quantitative performance assessment from dynamic analysis.

Structures incorporated with supplemental damping devices are a type of structure that has been established for use toward high-performance objectives to minimize post-earthquake disruption. Extensive research works have demonstrated that incorporating damping devices in structure design not only can reduce the engineering demand parameters (EDPs) that necessitate special attention in the design of nonstructural components, equipment, and contents, but also can reduce the structural material cost and carbon footprint of the structure [29–33]. The recent construction of The 181 Fremont tower in San Francisco demonstrates the rising trend of implementation of advanced damping technologies to enable the resilience-based design of buildings to achieve a "Gold" rating as outlined in the REDi Rating System [34]. With this rising trend of implementation, research works have reported one of the distinctive characteristics of structures with supplemental damping devices that needed to be considered in the

design and analysis of such types of structures, i.e., the dynamic properties of these structures are variable during the excitations of dynamic loadings. For instance, Sause et al. [35] revealed the dependence of near-optimal damping on brace stiffness for structures with viscoelastic dampers. Fu and Kasai [36] showed the stiffness and damping of viscoelastic and viscous damper systems depend not only on the type of damper but also on the mechanical interaction of the damper with the structure. Lin and Chopra [37] found the effectiveness of nonlinear dampers in structural response reduction depends on both bracing stiffness and spectral region of the pseudo-velocity response spectrum of ground motions. Dong et al. [38] experimentally observed the mechanism of dynamic stiffness of steel frame structures with nonlinear viscous dampers when subjected to ground motion excitations. In practice, despite seismic design provisions such as those ASCE/SEI 41-06 [39], FEMA P-750 [40], and ASCE/SEI 7-10 [41] have included analysis procedures to promote the use of supplemental damping technology in seismic-resistant design, the loading dependent characteristics of such type of structures has never been considered in the process of ground motion selection for use in dynamic analysis and performance assessment. Therefore, in order to reliably relate earthquake hazard measures to the performance of structures with supplemental damping devices, it's necessary to account for the variable dynamic properties of structures in ground motion selection.

This paper proposes a site-specific ground motion selection procedure, through which to implement the PBEE framework to relate earthquake hazard to structural performance for structures with variable dynamic properties using the context of a steel structure with supplemental damping devices at a paradigm building site. In Section 2, this paper begins by discussing the differences between the risk-target hazard from ASCE/SEI 7-10 seismic design maps and the site-specific hazard from PSHA, and assessing the suitability of ground motion selection approaches using the UHS and CMS as the target hazard spectrum for structures with variable dynamic properties. Based on this, Section 3presents a site-specific ground motion selection procedure using the target spectra of UHS. Then in Section 4, suits of ground motions representing various hazard intensity levels at a paradigm building site are selected for use in dynamic analysis of the reduced design of steel structure with supplemental damping devices. Section 5 presents the details of the design and modeling of the steel structure damped with nonlinear viscous dampers. Finally, an evaluation of the probability distribution of the major EDPs including peak story drift, residual story drift, peak floor velocity, and peak floor acceleration is given in Section 6. Through the evaluation, it is demonstrated that the proposed UHSbased site-specific ground motion selection procedure enabled the estimation of the major EDPs of the paradigm structure using a probabilistic approach, which is critical to the performance assessment of structures with variable dynamic properties in the PBEE framework.

2. Site-specific hazard and target hazard spectrum

2.1. Ground motion maps and site-specific hazard

Historically, the earthquake ground motion maps in the NEHRP Provisions and ASCE/SEI 7 Standards have been directly based on the National Seismic Hazard Models (NSHM) of the U.S. Geological Survey (USGS). Based on the 2008 update of the USGS NSHM for the conterminous United States [42], both the 2009 NEHRP Recommended Seismic Provisions and the 2010 ASCE/SEI 7-10 Standard contain maps of Risk-Targeted Maximum Considered Earthquake (MCE_R) spectral response accelerations at 0.2 s and 1.0 s, denoted S_S and S_1 , respectively, for designing buildings and other structures. This risk-targeted MCE_R spectral acceleration intensity was adopted to achieve a more uniform probability of collapse across various seismic zones within the U.S., recognizing the probability of collapse is not necessarily equal to the probability of the ground motion intensity exceeding the maximum considered earthquake (MCE) ground motion intensity which has a POE

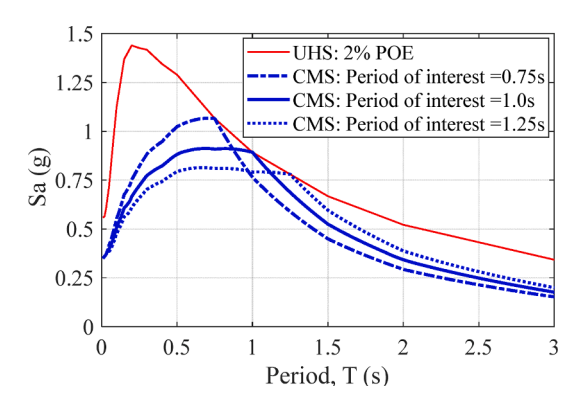
of 10% in 50 years. According to ASCE/SEI 7-10, the site-specific MCE_R spectral response acceleration at any period shall be taken as the lesser of the spectral response accelerations from the probabilistic ground motions and the deterministic ground motions. The probabilistic MCE_R spectral acceleration is defined as the spectral acceleration in the direction of the maximum horizontal response represented by a 5-percent damped acceleration response spectrum that is expected to result in a 1.0% probability of collapse within a 50-year period, while the deterministic MCE_R spectral acceleration is defined as the 84th-percentile 5-percent damped spectral acceleration in the direction of the maximum horizontal response.

For a paradigm building site in southern California (latitude, longitude = 33.979° N, 117.6° W; class D) with $S_S = 1.5$ g and $S_1 = 0.9$ g, both the MCE_R response spectrum and the design spectrum of ASCE/SEI 7-10 can be determined, as shown in Fig. 1. The design spectrum represents the design basis earthquake (DBE) hazard intensity which has a POE of 10% in 50 years. Also compared in the figure are the site-specific UHS generated by the USGS and the UHS for an arbitrary component of horizontal ground motions generated using the Campbell and Bozorgnia (2008) ground motion model [43], referred to herein as the CB08 model. The CB08 model is one of the equally-weighted three ground motion models that were implemented to generate the 2008 USGS seismic hazard maps for crustal faults in the Western United States (WUS) [42]. As can be seen, although the USGS site-specific UHS with 2% POE in 50 years and the MCE_R spectrum of ASCE/SEI 7-10 have comparable spectral accelerations at 0.2 s and 1.0 s, the discrepancies in spectral accelerations over the period range tell the difference between the sitespecific hazard and the hazard represented by the ASCE/SEI 7-10 Standard spectrum. However, the UHS generated using the CB08 model closely matches the USGS site-specific UHS for various hazard levels including the intensity with 2%, 10%, and 50% POE in 50 years. In this regard, for a specific site where the site-specific MCE_R spectral response acceleration is governed by the probabilistic MCE_R spectral, the UHS generated using the CB08 model can be used as the target hazard spectrum if the maximum structural response under an arbitrary ground motion component regardless of direction is of interest. The target UHS was generated using the OpenSHA program [44].

2.2. Target hazard spectrum

The objective of ground motion selection for a target hazard is to provide a reliable prediction of structural response through dynamic analysis. Thus, a target hazard spectrum to which the spectra of ground motions are matched is required. The UHS and CMS are two types of target hazard spectra that have been commonly used for ground motion selection in literature and practice. The UHS is an envelope of the spectral amplitudes at all periods that have the same POE (e.g., 50%, 10%, and 2% in 50 years) that are computed using the PSHA, which hypothetically does not undervalue the hazard for a specific site of interest. Though the UHS is not a genuine representative of the spectral shape of any single ground motion, it has been legitimately replicated by

the design spectra in seismic design provisions for use in seismic design. On the other hand, as the CMS is constructed on the condition of a given target spectral acceleration value for a specified hazard at a period of interest, it is regarded as the expected response spectrum for ground motions [22]. The conditional period of interest for the CMS is usually the fundamental period of the structure or the period at which the structure has a dominant dynamic response. If a structure has a dominant dynamic response at multiple periods, or if the period corresponding to the dominant structural response is indeterminate due to variable dynamic characteristics under transit ground motion excitations, multiple CMS target hazard spectra corresponding to multiple periods of interest need to be considered. This dilemma poses a challenge for selecting ground motions to a CMS target hazard spectrum for structures with variable dynamic properties such as structures with supplemental damping devices of which the structural behavior is sensitive to loading rate. For instance, Dong et al. [38] observed that the identified first mode frequencies of structures with nonlinear viscous dampers under the DBE and MCE ground motion excitations are 20% ~75% higher than the frequencies of the structures at rest, depending on the supplemental damping level. Fig. 2 shows the comparison of the UHS with the CMS conditioned on multiple periods of interest. As can be seen, the spectral accelerations of a CMS conditioned on a shorter period of interest (e.g., 0.75 s) are larger than those of a CMS conditioned on a longer period of interest (e.g., 1.25 s) when the spectral periods are less than 1.0 s, and smaller when the spectral periods are greater than 1.0 s. Due to this challenge for implementing the CMS for ground motion selection for structures sensitive to dynamic excitation at multiple periods, epistemic uncertainty could arise in the observations of structural response from dynamic analysis if ground motions are selected based on the CMS that is conditioned on a longer period of interest than the fundamental period of the structure. In the meantime, although the UHS is not a genuine representative of the spectral shape of any single ground motion, it is less likely to undervalue the hazard at a specific site. Therefore, this study uses the UHS rather than the CMS as the target hazard spectrum for ground motion selection for structures with



 $\textbf{Fig. 2.} \ \ \textbf{Comparison of UHS and CMS target hazard spectra.}$

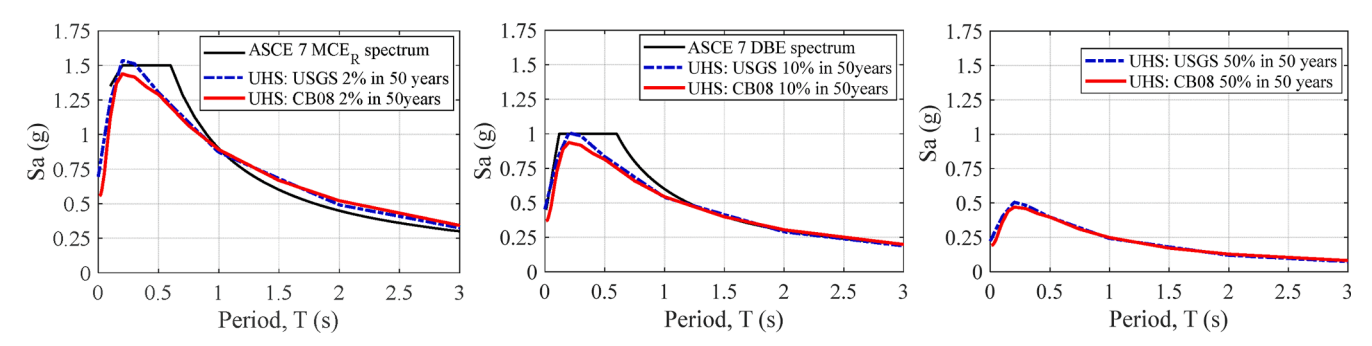


Fig. 1. ASCE/SEI 7-10 MCE_R spectrum, design spectrum, and uniform hazard spectrum.

variable dynamic properties (i.e., structures with supplemental damping devices. Correspondingly, a procedure for ground motion selection for such structures with damping devices at a specific site is developed in Section 3.

3. Site-specific ground motion selection procedure for damped structures

The procedure for selecting and scaling ground motions for a specific seismic hazard level represented by the UHS at the building site has the following steps:

Step 1: Characterize site-specific seismic hazard. The seismic hazard at the building site should be characterized by performing PSHA. The USGS Seismic Hazard Maps and Site-Specific Data tool (https://www.usgs.gov/programs/earthquake-hazards/seismic-hazard-maps-and-site-specific-data) or the ASCE/SEI 7 hazard tool (https://asce7hazardtool.online/) can be used to understand the hazard at a specified period, i.e., spectral response accelerations at 0.2 s and 1.0 s. The USGS site-specific UHS at the building site should be compared to the ASCE/SEI 7 spectrum, as like in Fig. 1, to discern the compatibility and discrepancy between the site-specific hazard and the mapped hazard in ASCE/SEI 7.

Step 2: Establish the target hazard spectrum. As the maximum structural response under an arbitrary ground motion component, regardless of direction, is of interest to the evaluation of engineering demand parameters, the mapped spectral response accelerations in ASCE /SEI 7-10 are maximum horizontal response direction based for buildings. Thus, the UHS for an arbitrary component of horizontal ground motions generated using the CB08 ground motion model [43] can be used as the target hazard spectrum. Compared to other ground motion models used in the USGS [45–46], the Campbell and Bozorgnia model is able to predict the arbitrary horizontal component of ground motions. The OpenSHA program [44] can be used to generate the target UHS. As shown in Fig. 1, the predicted target hazard spectrum shall be compared to the USGS site-specific UHS and the spectrum in ASCE/SEI 7-10 for various hazard levels, respectively.

Step 3: Hazard deaggregation. The contributions to the hazard from various magnitude (M), distance (R), and epsilon (ε) combinations can be calculated through the deaggregation of hazard. The epsilon (ε), defined by Baker et al [21], is an indication of the shape of the response spectrum for a ground motion. The deaggregation represents the conditional probability of M, R and ε when the spectral acceleration exceeds the hazard level at the building site. For instance, the mean M, R, and ε for the target hazard with 2% POE in 50 years at period range from 0.1 to 3.0 s at for the sleeted paradigm building site (i.e., site latitude, longitude = 33.979° N, 117.6° W) can be obtained, which are listed in Table 1. The mean earthquake magnitudes for the hazards at 0.2 s and 1.0 s are $M_{\rm W}$ 6.62 and $M_{\rm W}$ 7.17, respectively.

Step 4: Ground motion amplitude scaling. Earthquake ground motion records from the PEER NGA Database [47] can be selected and scaled to match the target UHS over a period range from $0.2\,s$ to $4.0\,s$. The PEER NGA database consists of 3551 multi-component records from 173 shallow crustal earthquakes with magnitudes ranging from 4.2 to

Table 1Mean magnitude, distance, and epsilon from deaggregation of hazard with 2% POE in 50 years at paradigm building site.

Period, T (s)	Spectral acceleration, Sa (g)	Magnitude, $M_{\rm w}$	Distance, <i>R</i> (kM)	Epsilon, ε
0.1	1.22	6.54	15.6	1.70
0.2	1.51	6.62	16.2	1.73
0.3	1.48	6.73	17.1	1.72
0.5	1.27	6.87	17.9	1.72
1.0	0.87	7.17	21.4	1.79
2.0	0.49	7.44	26.4	1.76
3.0	0.33	7.58	28.3	1.68

7.9. The scale factor for each record is calculated using Equation (1):

$$scale\ factor = \frac{\sum_{j=1}^{n} S_a^{\text{target}}(T_j)}{\sum_{i=1}^{n} S_a^{\text{record}}(T_i)}$$
 (1)

where $S_a^{\rm record}(T_j)$ is the spectral acceleration of the ground motion at period T_j , $S_a^{\rm target}(T_j)$ is the spectral acceleration of the target UHS at period T_j , and n is the number of periods used for the calculation. A total of 16 periods (i.e., n=16) in the range of 0.2 to 4.0 s (i.e., 0.2, 0.25, 0.3, 0.4, 0.5, 0.6, 0.75, 0.85, 1.0, 1.2, 1.5, 2.0, 2.5, 3.0, 3.5, and 4.0 s) are recommended to use in the calculation.

Step 5: Matching indicator calculation. The match between each scaled ground motion record and the target hazard spectrum is quantified by the sum of squared errors (SSE) [22], as Equation (2). A smaller SSE indicates the scaled ground motion record more closely matches the target hazard spectrum over the period range of interest.

$$SSE = \sum_{j=1}^{n} \left(\ln S_a^{\text{record}}(T_j) - \ln S_a^{\text{target}}(T_j) \right)^2$$
 (2)

where $\ln S_a^{\rm record}(T_j)$ is the logarithm of the spectral acceleration of the ground motion record at period T_j , and $\ln S_a^{\rm target}(T_j)$ is the logarithm of the spectral acceleration of the target UHS at period T_j . The 16 periods used for the scale factor calculation are also used for the *SSE* calculation. The logarithm of the spectral acceleration is used in Equation (2) based on an assumption of lognormal distribution for the spectral accelerations of ground motions at each period. Eventually, the median spectral acceleration spectrum of the selected suite of ground motions can be obtained using Equation (3), which is expected to match the target UHS.

$$S_a^{\text{median}} = e^{\frac{1}{N} \sum_{i=1}^{N} \ln S_a^{\text{record}}(i)}$$
(3)

where N is the total number of individual ground motions included in the selected suite of ground motions, $S_a^{\rm record}(i)$ is the spectral acceleration of the $i^{\rm th}$ individual ground motion, and $S_a^{\rm median}$ is the median spectral acceleration of the suite of ground motions.

Step 6: Ground motion refinement. Depending on the number of records desired to be included in the selected suite of ground motions, records with smaller SSE values should be included with priority. To better represent the hazard events sources at the building site, each suite of ground motions should be refined by only including the ground motions with magnitudes and distances that are close to the deaggregation results. Ground motions with large scale factors, with spectral shapes that are significantly different than the target UHS, and without detailed information about the recording stations, should be excluded from the ground motion suite.

4. Paradigm building site and ground motions

A stiff soil site, where the hazard from PSHA is consistent with the hazard represented by the ASCE/SEI 7-10 seismic maps, is selected as the paradigm building site for this study. The site is located in Pomona, California (latitude, longitude = 33.979° N, 117.6° W). According to USGS, the spectral acceleration at 0.2 s and 1.0 s at this site are $S_s = 1.51$ g and $S_1 = 0.87$ g for hazard intensity with 2% POE in 50 years (i.e., the MCE level intensity with a return period of 2475 years) (see Fig. 3) and $\textit{S}_{\textrm{s}} = 1.01$ g and $\textit{S}_{\textrm{1}} = 0.54$ g for hazard intensity with 10% POE in 50 years (i.e., the DBE level intensity with a return period of 475 years). These values are substantially close to the values of $S_s = 1.5$ g and $S_1 =$ 0.9 g for the MCE response spectrum and $S_s = 1.0$ g and $S_1 = 0.6$ g for the DBE response spectrum from ASCE/SEI 7–10. As illustrated in Fig. 1, the site-specific UHS generated using the CB08 ground motion model are compared with the response spectrum from ASCE/SEI 7-10 and the UHS generated by the USGS for POE of 10% and 2% in 50 years, respectively. These plots show the discrepancies in spectral accelerations of these

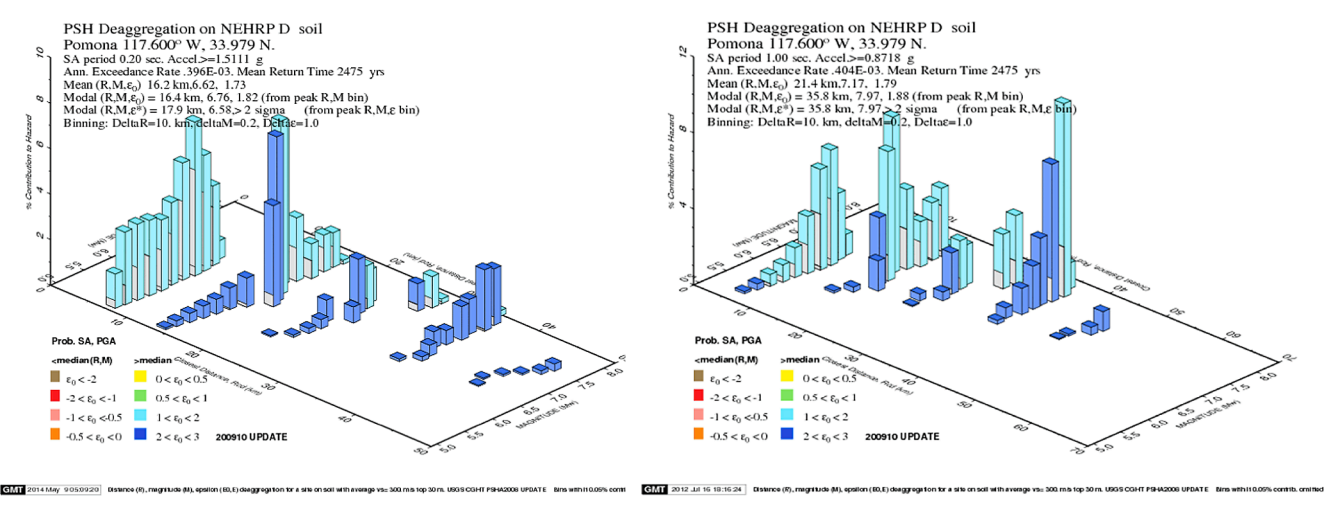


Fig. 3. PSHA deaggregation of hazard with 2% POE in 50 years at 0.2 s and 1.0 s for the paradigm building site (USGS Unified Hazard Tool, https://earthquake.usgs.gov/hazards/interactive/).

spectra are small for the paradigm site.

Using the procedure in Section 3, three suites of 40 ground motions were selected to represent the frequently occurring earthquake (FOE) which has a POE of 50% in 50 years, DBE, and MCE hazard levels at the building site. Detailed information for the suites of ground motions are

summarized in Tables 2, 3 and Table 4. The response spectra for these ground motions, the median spectrum of the ground motions, and the target hazard spectrum are plotted in log scale and compared in Fig. 4. As can be seen, the median spectrum of each ground motion suite has good agreement with the target spectrum over the period range of 0.1 s

Table 2
Ground motions at FOE hazard level.

ID	NGA Record No.	Earthqual	ke					Ground motion record	Scale Factor	SSE	
		R (kM)	M_{w}	ε	Vs30 (m/s)	Year	Name				
1	832	69.2	7.3	0.37	271.4	1992	Landers	ABY000	1.48	0.74	
2	832	69.2	7.3	0.44	271.4	1992	Landers	ABY090	1.30	0.63	
3	949	8.7	6.7	1.30	297.7	1994	Northridge	ARL360	0.75	0.84	
4	721	18.2	6.5	1.55	192.1	1987	Superstition Hills	B-ICC000	0.63	0.79	
5	138	28.8	7.4	0.24	338.6	1978	TABAS	BOS-L1	1.71	0.61	
6	838	34.9	7.3	0.48	370.8	1992	Landers	BRS000	1.64	1.00	
7	728	13.0	6.5	0.56	193.7	1987	Superstition Hills	B-WSM090	1.04	0.58	
8	1181	47.3	7.6	0.14	271.3	1999	Chi-Chi, Taiwan	CHY004-N	1.86	0.61	
9	1208	24.1	7.6	1.15	442.2	1999	Chi-Chi, Taiwan	CHY046-N	0.91	0.33	
10	1236	37.5	7.6	1.07	272.6	1999	Chi-Chi, Taiwan	CHY088-E	1.03	0.79	
11	1042	12.5	6.7	0.83	446	1994	Northridge	CWC270	0.78	0.62	
12	850	21.8	7.3	1.20	345.4	1992	Landers	DSP090	1.10	1.22	
13	1605	6.6	7.1	2.81	276	1999	Duzce, Turkey	DZC270	0.35	0.52	
14	161	10.4	6.5	0.87	208.7	1979	Imperial Valley	H-BRA315	0.85	0.56	
15	334	42.0	6.4	0.19	338.5	1983	COALINGA	H-COW090	1.29	0.94	
16	778	24.8	6.9	1.73	215.5	1989	Loma Prieta	HDA165	0.63	1.06	
17	169	22.0	6.5	1.39	274.5	1979	Imperial Valley	H-DLT262	0.72	0.79	
18	169	22.0	6.5	1.66	274.5	1979	Imperial Valley	H-DLT352	0.58	0.57	
19	178	12.9	6.5	1.32	162.9	1979	Imperial Valley	H-E03140	0.68	0.63	
20	175	17.9	6.5	0.13	196.9	1979	Imperial Valley	H-E12140	1.39	0.51	
21	170	7.3	6.5	1.47	192.1	1979	Imperial Valley	H-ECC002	0.69	1.18	
22	1810	92.0	7.1	0.96	345.4	1999	Hector Mine	HECTOR-11625090	1.35	1.11	
23	1762	43.1	7.1	1.06	271.4	1999	Hector Mine	HECTOR-21081360	1.13	0.54	
24	185	7.7	6.5	1.22	202.9	1979	Imperial Valley	H-HVP225	0.74	1.19	
25	776	27.9	6.9	0.93	370.8	1989	Loma Prieta	HSP090	0.81	0.87	
26	1009	23.6	6.7	0.76	392.2	1994	Northridge	NORTH5082A-235	0.91	0.92	
27	316	16.7	5.9	1.44	348.7	1979	Westmorland	PTS315	0.89	0.46	
28	1085	5.2	6.7	3.23	370.5	1994	Northridge	SCE018	0.28	0.41	
29	787	30.9	6.9	1.46	425.3	1989	Loma Prieta	SLC270	0.79	1.15	
30	787	30.9	6.9	1.30	425.3	1989	Loma Prieta	SLC360	0.64	1.23	
31	802	8.5	6.9	1.60	370.8	1989	Loma Prieta	STG000	0.58	1.01	
32	1481	25.4	7.6	1.06	272.6	1999	Chi-Chi, Taiwan	TCU038-N	0.82	0.59	
33	1484	26.3	7.6	1.08	272.6	1999	Chi-Chi, Taiwan	TCU042-E	0.89	0.28	
34	1490	9.5	7.6	0.96	272.6	1999	Chi-Chi, Taiwan	TCU050-E	1.03	0.63	
35	1491	7.7	7.6	0.88	272.6	1999	Chi-Chi, Taiwan	TCU051-E	0.92	0.74	
36	1495	6.4	7.6	1.45	272.6	1999	Chi-Chi, Taiwan	TCU055-E	0.67	0.48	
37	1546	9.4	7.6	1.23	475.5	1999	Chi-Chi, Taiwan	TCU122-N	0.74	0.61	
38	1008	29.7	6.7	0.15	405.2	1994	Northridge	W15090	1.56	0.80	
39	803	9.3	6.9	2.15	370.8	1989	Loma Prieta	WVC270	0.52	1.17	
40	900	23.6	7.3	0.89	353.6	1992	Landers	YER360	0.97	0.73	

Table 3Ground motions at DBE hazard level.

ID	NGA Record No.	Earthqual	ke				Ground motion record	Scale Factor	SSE		
		R (kM) M _w		v ε Vs30 (m/s)		Year	Name				
1	721	18.2	6.5	1.27	192.1	1987	Superstition Hills	B-ICC000	1.33	1.22	
2	729	23.9	6.5	1.27	207.5	1987	Superstition Hills	B-IVW360	1.30	0.87	
3	725	11.2	6.5	0.89	207.5	1987	Superstition Hills	B-POE360	1.52	0.81	
4	1208	24.1	7.6	0.87	442.2	1999	Chi-Chi, Taiwan	CHY046-N	1.94	0.59	
5	1209	24.1	7.6	0.75	272.6	1999	Chi-Chi, Taiwan	CHY047-N	2.04	0.65	
6	1042	12.5	6.7	0.55	446	1994	Northridge	CWC270	1.66	0.85	
7	850	21.8	7.3	0.91	345.4	1992	Landers	DSP090	2.34	1.65	
8	1158	15.4	7.5	1.24	276	1999	Kocaeli, Turkey	DZC180	1.19	1.27	
9	1605	6.6	7.1	2.53	276	1999	Duzce, Turkey	DZC270	0.74	0.39	
10	161	10.4	6.5	0.59	208.7	1979	Imperial Valley	H-BRA315	1.80	1.03	
11	778	24.8	6.9	1.45	215.5	1989	Loma Prieta	HDA165	1.33	1.03	
12	169	22.0	6.5	1.10	274.5	1979	Imperial Valley	H-DLT262	1.52	0.94	
13	169	22.0	6.5	1.38	274.5	1979	Imperial Valley	H-DLT352	1.24	0.82	
14	178	12.9	6.5	1.04	162.9	1979	Imperial Valley	H-E03140	1.44	0.44	
15	1810	92.0	7.1	0.67	345.4	1999	Hector Mine	HECTOR-11625090	2.88	0.77	
16	1762	43.1	7.1	0.77	271.4	1999	Hector Mine	HECTOR-21081360	2.41	0.43	
17	185	7.7	6.5	0.94	202.9	1979	Imperial Valley	H-HVP225	1.56	0.87	
18	776	27.9	6.9	0.64	370.8	1989	Loma Prieta	HSP090	1.72	0.82	
19	1013	5.9	6.7	1.74	629	1994	Northridge	LDM334	1.09	0.48	
20	316	16.7	5.9	1.16	348.7	1979	Westmorland	PTS315	1.88	0.41	
21	1063	6.5	6.7	2.25	282.3	1994	Northridge	RRS318	0.66	1.64	
22	1085	5.2	6.7	2.95	370.5	1994	Northridge	SCE018	0.59	0.52	
23	1085	5.2	6.7	2.29	370.5	1994	Northridge	SCE288	0.81	1.24	
24	787	30.9	6.9	1.18	425.3	1989	Loma Prieta	SLC270	1.67	1.17	
25	787	30.9	6.9	1.02	425.3	1989	Loma Prieta	SLC360	1.35	1.74	
26	1481	25.4	7.6	0.78	272.6	1999	Chi-Chi, Taiwan	TCU038-N	1.74	0.66	
27	1484	26.3	7.6	0.80	272.6	1999	Chi-Chi, Taiwan	TCU042-E	1.68	0.36	
28	1484	26.3	7.6	0.80	272.6	1999	Chi-Chi, Taiwan	TCU042-N	1.81	1.01	
29	1490	9.5	7.6	0.67	272.6	1999	Chi-Chi, Taiwan	TCU050-E	2.18	0.35	
30	1491	7.7	7.6	0.60	272.6	1999	Chi-Chi, Taiwan	TCU051-E	1.95	0.42	
31	1495	6.4	7.6	1.17	272.6	1999	Chi-Chi, Taiwan	TCU055-E	1.41	0.46	
32	1495	6.4	7.6	0.84	272.6	1999	Chi-Chi, Taiwan	TCU055-N	1.59	0.99	
33	1496	10.5	7.6	0.66	272.6	1999	Chi-Chi, Taiwan	TCU056-E	2.09	0.80	
34	1496	10.5	7.6	0.77	272.6	1999	Chi-Chi, Taiwan	TCU056-N	2.15	0.91	
35	2655	19.3	6.2	0.63	475.5	1999	Chi-Chi, Taiwan	TCU122-E	2.09	1.04	
36	1546	9.4	7.6	0.95	475.5	1999	Chi-Chi, Taiwan	TCU122-N	1.56	0.37	
37	803	9.3	6.9	1.44	370.8	1989	Loma Prieta	WVC000	1.25	1.40	
38	803	9.3	6.9	1.87	370.8	1989	Loma Prieta	WVC270	1.11	0.91	
39	900	23.6	7.3	1.15	353.6	1992	Landers	YER270	1.47	1.21	
40	900	23.6	7.3	0.60	353.6	1992	Landers	YER360	2.06	0.83	

to 4.0 s for each hazard level. Fig. 5 shows the lognormal standard deviations of spectral accelerations of the ground motions varying over the spectral periods. The average lognormal standard deviation is approximately 0.25 over the period range from 0.2 s to 3.0 s for each ground motion suite, indicating the ground motions are fairly well matched to the target hazard spectrum. Therefore, it would be reliable to use these ground motions in time history dynamic analysis for engineering demands prediction and seismic performance evaluation.

5. Design and modeling of prototype structure

5.1. Design of prototype structure

A typical three-story office building structure located on the paradigm site is chosen for this study. For the seismic resistant design of the building according to ASCE/SEI 7–10, moment resisting frames (MRFs) are used as the lateral force resisting system, while damped brace frames (DBFs) are used as the supplemental damping system. Large force capacity nonlinear viscous dampers with velocity exponent $\alpha=0.44$ were used in the DBFs. Fig. 6(a) shows the six-bay by eight-bay floor plan of the building. A total of eight identical pairs of single-bay MRF and DBF, with four pairs in each horizontal direction, are distributed in the perimeter of the building. The pairs of MRF and DBF work in parallel in the same direction through the action of the floor diaphragm that transfers the earthquake-induced inertial forces into the MRFs and DBFs. Thus, a pair of MRF and DBF in one direction is studied herein as the

prototype structure, as shown in Fig. 6(b). The seismic tributary area for the prototype structure is one-quarter of the total building area (i.e., three-bay by four-bay).

A performance-based design approach is used for the integrated design between the MRF (i.e., the LFRS) and the DBF (i.e., supplemental damping system) of the prototype structure for desired performance objectives [48]. According to the requirement of ASCE/SEI 7-10, the MRF is designed for a minimum strength level, that is, the 75% of the base shear strength demand determined from the equivalent lateral force (ELF) procedure with parameters R = 8, $C_d = 5.5$, $S_{DS} = 1.0$ g, S_{D1} = 0.6 g. Therefore, the MRF is referred to as a reduced strength design of MRF in this study. Given the design strength, the MRF is sized according to AISC 360-10 [49] and AISC 341-10 [50], using wide flange sections with ASTM A992 steel for the beams and columns. Also, reduced beam sections are used in the MRF to protect the beam-to-column welded connections. As the supplemental damping system of the structure, the members of the DBF are sized to supposedly remain elastic when subjected to the DBE level ground motions. Considering the practical availability of nonlinear viscous dampers with a force capacity of 600 kN and the need to use the same structure for large-scale experimental study [33], the pair of MRF and DBF are downsized with a scale factor of 0.6 for this study, as shown in Fig. 6(b) for the elevation view. As can be seen, the structure is horizontally restrained at the ground level, and the columns of the MRF and DBF are pinned at the column base. Chevron diagonal braces are used to connect the damper to the floors in each story of the DBF. The gravity system tributary to the MRF and DBF is

Table 4Ground motions at MCE hazard level.

ID	NGA RecordNo.	Earthqual	ke					Ground motion record	Scale Factor	SSE
		R (kM)	M_{w}	ε	Vs30 (m/s)	Year	Name			
1	729	23.9	6.5	1.28	207.5	1987	Superstition Hills	B-IVW360	2.09	0.62
2	725	11.2	6.5	0.90	207.5	1987	Superstition Hills	B-POE360	2.44	1.12
3	1208	24.1	7.6	0.73	442.2	1999	Chi-Chi, Taiwan	CHY046-N 3.12		0.83
4	1042	12.5	6.7	1.33	446	1994	Northridge	CWC270	2.67	1.08
5	850	21.8	7.3	0.86	345.4	1992	Landers	DSP090	3.77	1.96
6	1158	15.4	7.5	1.27	276	1999	Kocaeli, Turkey	DZC180	1.91	1.14
7	1605	6.6	7.1	1.69	276	1999	Duzce, Turkey	DZC270	1.19	0.41
8	161	10.4	6.5	0.67	208.7	1979	Imperial Valley	H-BRA315	2.89	1.37
9	778	24.8	6.9	0.82	215.5	1989	Loma Prieta	HDA165	2.15	1.09
10	169	22.0	6.5	0.39	274.5	1979	Imperial Valley	H-DLT262	2.45	1.10
11	169	22.0	6.5	1.44	274.5	1979	Imperial Valley	H-DLT352	1.99	1.04
12	178	12.9	6.5	0.46	162.9	1979	Imperial Valley	H-E03140	2.31	0.46
13	170	7.3	6.5	1.23	192.1	1979	Imperial Valley	H-ECC002	2.35	1.43
14	170	7.3	6.5	0.95	192.1	1979	Imperial Valley	H-ECC092	2.44	1.42
15	1762	43.1	7.1	0.28	271.4	1999	Hector Mine	HECTOR-21081090	3.65	1.13
16	1794	31.1	7.1	0.75	379.3	1999	Hector Mine	HECTOR-22170090	4.27	2.54
17	185	7.7	6.5	0.83	202.9	1979	Imperial Valley	H-HVP225	2.52	0.79
18	185	7.7	6.5	0.63	202.9	1979	Imperial Valley	H-HVP315	2.87	1.92
19	776	27.9	6.9	2.58	370.8	1989	Loma Prieta	HSP000	1.26	2.86
20	776	27.9	6.9	1.20	370.8	1989	Loma Prieta	HSP090	2.76	0.87
21	864	11.0	7.3	1.46	379.3	1992	Landers	JOS090	1.92	1.87
22	1010	23.6	6.7	1.13	413.8	1994	Northridge	NORTHR-5082-235	2.91	2.28
23	316	16.7	5.9	0.76	348.7	1979	Westmorland	PTS315	3.03	0.47
24	1063	6.5	6.7	2.03	282.3	1994	Northridge	RRS318	1.07	1.93
25	1085	5.2	6.7	0.96	370.5	1994	Northridge	SCE018	0.95	0.67
26	1085	5.2	6.7	2.63	370.5	1994	Northridge	SCE288	1.30	1.31
27	802	8.5	6.9	1.29	370.8	1989	Loma Prieta	STG000	1.97	1.71
28	802	8.5	6.9	1.05	370.8	1989	Loma Prieta	STG090	2.78	1.36
29	1077	26.5	6.7	1.11	336.2	1994	Northridge	STM360	2.62	2.40
30	1484	26.3	7.6	0.64	272.6	1999	Chi-Chi, Taiwan	TCU042-E	2.69	0.51
31	1491	7.7	7.6	1.07	272.6	1999	Chi-Chi, Taiwan	TCU051-E	3.15	0.35
32	1495	6.4	7.6	0.92	272.6	1999	Chi-Chi, Taiwan	TCU055-N	2.57	0.73
33	1496	10.5	7.6	0.76	272.6	1999	Chi-Chi, Taiwan	TCU056-E	3.36	0.59
34	1496	10.5	7.6	0.40	272.6	1999	Chi-Chi, Taiwan	TCU056-N.at2	3.46	0.67
35	1546	9.4	7.6	0.28	475.5	1999	Chi-Chi, Taiwan	TCU122-E.at2	3.01	0.97
36	1045	5.5	6.7	1.56	285.9	1994	Northridge	WPI316.at2	1.72	1.49
37	803	9.3	6.9	1.55	370.8	1989	Loma Prieta	WVC000.at2	2.02	1.52
38	803	9.3	6.9	1.85	370.8	1989	Loma Prieta	WVC270.at2	1.78	0.85
39	900	23.6	7.3	1.67	353.6	1992	Landers	YER270.at2	2.37	1.19
40	900	23.6	7.3	0.96	353.6	1992	Landers	YER360.at2	3.31	0.98

represented by a lean-on column with lumped masses and gravity loads at each floor level. The resulting 0.6-scaled prototype structure of MRF and DBF without dampers (hereinafter referred to as the undamped structure) has a fundamental period of 1.02 s, with story drift design predictions of 2.62% and 3.93% under the DBE and MCE level, respectively. For the structure including the MRF and DBF with dampers (hereinafter referred to as the damped structure), the equivalent viscous damping ratios (ξ_e) provided by the dampers are estimated using the lateral force energy (LFE) method [35], which are 35% and 26% under the DBE and MCE, respectively. The corresponding story drift predictions of the damped structure are 1.25% and 2.05% under the DBE and MCE, respectively. The reductions in story drifts by incorporating dampers into the structure are 52% and 48% under the DBE and MCE, respectively.

5.2. Modeling of prototype structure

To quantity the response of the structure under the selected ground motions with various intensities, a nonlinear numerical model of the structure is developed using the program OpenSees [51] for time history dynamic analysis. The beams and columns of the MRF and DBF are modeled using nonlinear beam-column fiber element. The nonlinear beam-column fiber element is based on a force formulation (i.e., flexibility based formulation) which considers the spread of plasticity distributed along the length of the element. The integration along the element is based on the Gauss-Lobatto quadrature rule. Each column in

each story of the MRF and DBF is modeled with one element. Due to the use of reduced beam sections at the ends of the beam in each story of the MRF, each beam in the MRF is modeled with 14 elements to better model the plasticity distribution at the ends of the beam. Seven fiber sections (i.e., integration points) are used along the length of these elements. Each fiber section is discretized into 22 fibers, with 12 fibers for the web and 5 fibers for each flange of the wide-flange steel sections. The axial force-deformation and moment-curvature response of each fiber section is accounted for by integrating the material stress-strain relationship from each fiber to give the resultant section behavior. The shear force-deformation response is accounted for by a shear force-shear deformation response associated with the fiber section. The "Steel01" material, which has a uniaxial bilinear stress-strain relationship with strain hardening, is used for the fibers at each section. The panel zone elements are used to model the shear deformation and uniform bending deformation of the panel zones of the beam-to-column connections. The elastic modulus and yielding stress of the material are 200,000 MPa and 345 MPa, respectively, and the strain hardening ratio (i.e., the ratio of the post-yielding modulus over the elastic modules) is 0.01. For the DBF, the chevron diagonal braces are modeled with linear elastic beamcolumn elements. The clevis connections that connect the damper to the braces and floor beams are modeled using the panel-zone elements to include shear deformation and uniform bending deformation of the panel zones of these components. The nonlinear viscous dampers are modeled using the Nonlinear Maxwell damper model [52]. The nonlinear Maxwell damper model, which consists of a nonlinear elastic

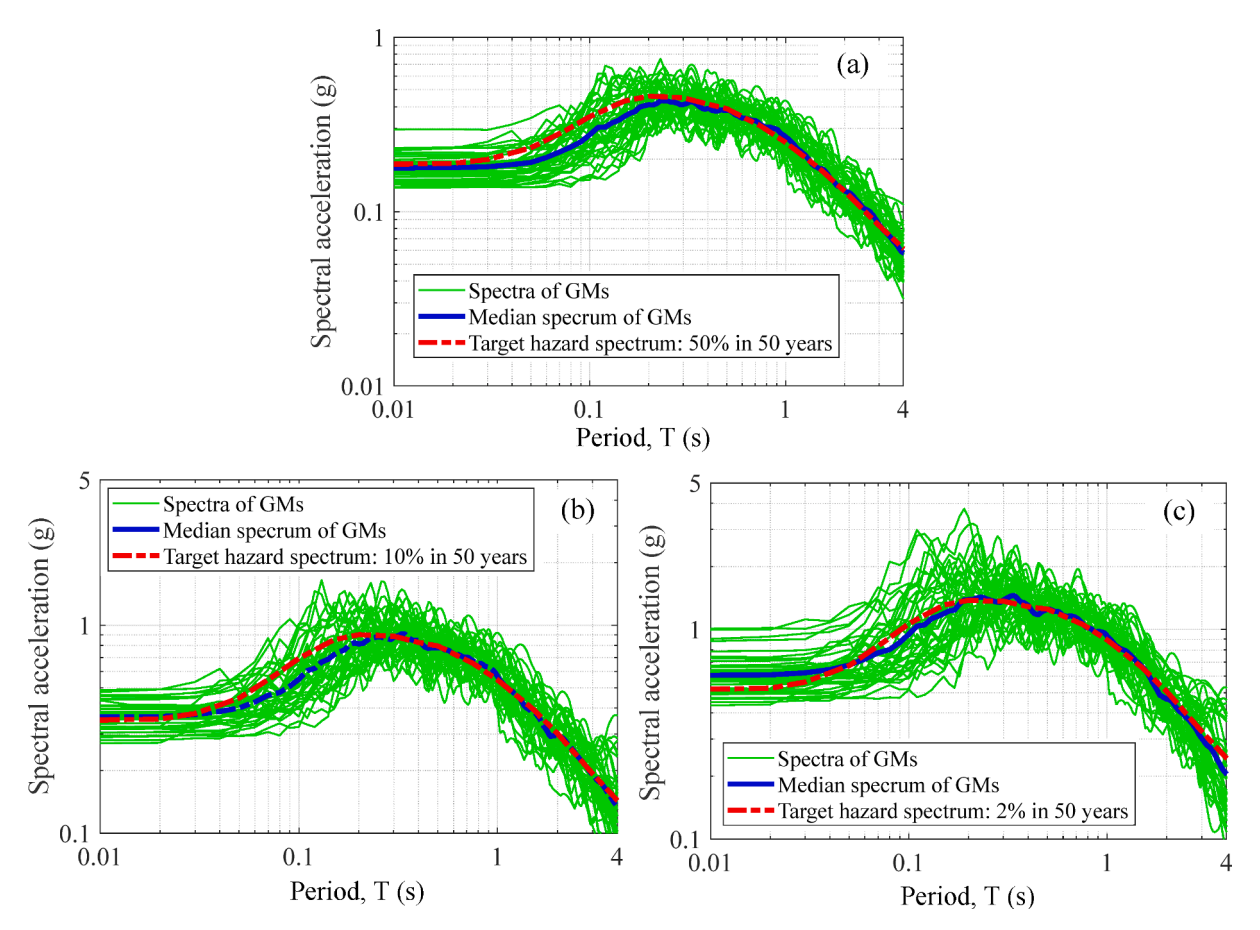


Fig. 4. Spectra and median spectrum of ground motions at various hazard levels: (a) FOE; (b) DBE; (c) MCE.

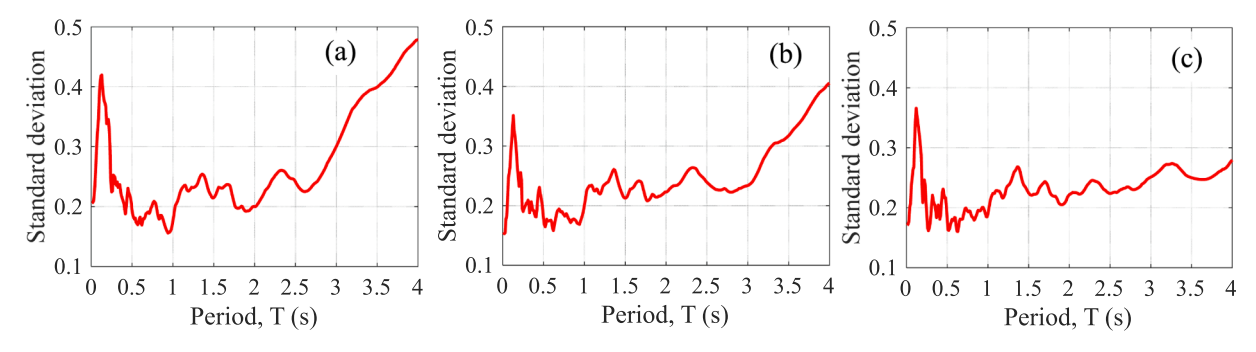


Fig. 5. Lognormal standard deviations of the spectral accelerations of ground motions versus spectral period: (a) FOE; (b) DBE; (c) MCE.

spring and a nonlinear dashpot connected in series, was validated to provide a simulated damper response that matches well with the damper response obtained from the characterization tests [53]. This damper model is implemented in OpenSees as a new uniaxial material using a zero-length element to represent the force-deformation and force-velocity response quantities of a nonlinear viscous damper.

To account for the P- Δ effects due to the gravity loads, a lean-on column is included in the model to simulate the gravity system in the seismic tributary area of a pair of MRF and DBF. The lean-on column is pinned at the ground level and modeled with one elastic beam-column element in each story of the structure. Gravity loads are applied at each floor level to introduce P- Δ effects into the model. In OpenSees, the geometric nonlinearity of the elements is included by using the corotational geometric transformation for the lean-on column elements. The seismic masses for the structure are the effective seismic weight of the seismic tributary area of a pair of MRF and DBF, divided by the

acceleration of gravity. In the model, the masses are assigned to the nodes of the lean-on column. To model an assumed rigid floor diaphragm, the nodes at 1/2 and 2/3 span and the top flange of the floor beams of the MRF and DBF are slaved to the nodes of the lean-on column at each floor level. This model transfers the inertial forces due to the floor masses on the lean-on column into the MRF and DBF. The inherent damping used in the model represents the energy dissipation characteristics of the building during low-amplitude dynamic response. The inherent damping is modeled using Rayleigh damping. The Rayleigh damping model is based on a 2% damping ratio for the first and second modes of the prototype structure. To account for the nonlinear behavior of the structure, the Newmark constant average acceleration method [54] and the modified Newton-Raphson iteration method were used to integrate the equations of motion of the numerical model. Iteration terminates when the incremental displacement becomes small enough, which is judged by the Euclidean norm of the incremental displacement

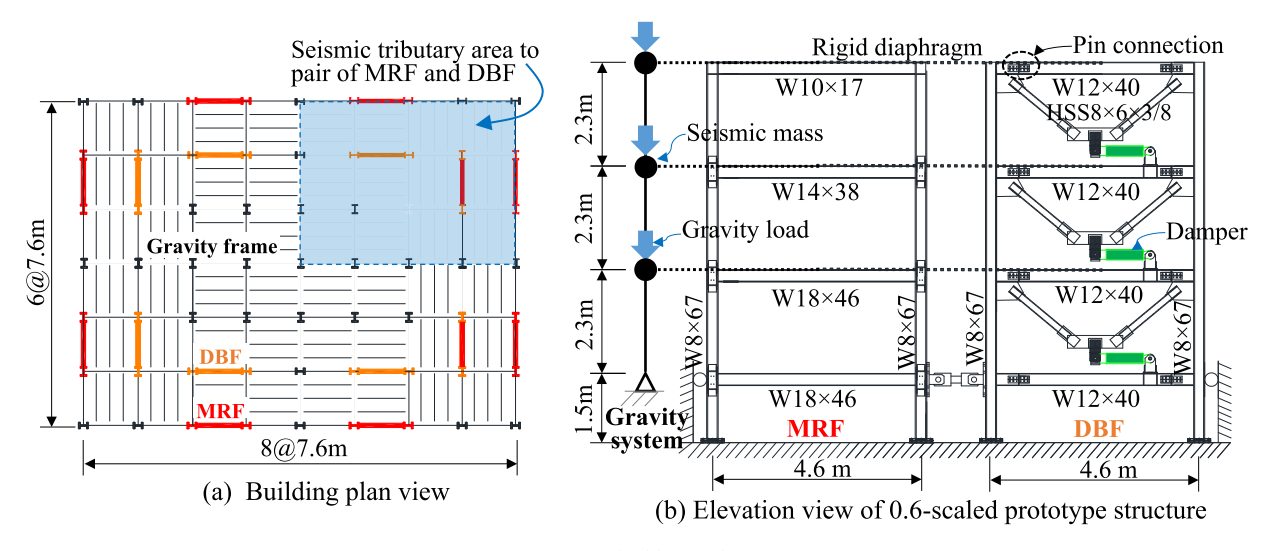


Fig. 6. Prototype building and structure.

to be smaller than 1×10^{-8} .

6. Observations and quantification of seismic response

6.1. Reduction in structural EDPs

The EDPs that can be used to predict damages to structural and nonstructural components such as peak story drift, residual story drift, peak floor velocity, peak absolute floor acceleration, and peak base shear are evaluated herein. The absolute floor acceleration response is obtained as the summation of the relative floor acceleration response and the ground acceleration. Tables 5-7 summarize the mean and coefficient of variance (CoV) values of the EDPs from the dynamic analysis of the undamped and damped structures with the selected suites of FOE, DBE, and MCE ground motions. The EDPs of the undamped and damped structures are compared to assess the effectiveness of the dampers in reducing the quantities of the EDPs and enhancing the resilience of the structure. Overall, the CoV values suggest the dispersion in the residual story drift response is larger than that in other EDPs. The reason is that the residual story drift response of a structure is not only largely dependent on its elasto-plastic behavior that is closely associated with the intensity of the ground motions, but also dependent on the time history characteristics of the ground motions. When yielding occurred to the structure at a moderate hazard level (e.g., the damped structure at the DBE hazard level) or the structure had been substantially yielded at a severe hazard level (e.g., the undamped structure at the MCE hazard level), due to a widespread observation of the residual story drift response, the dispersion in the residual story drift response of the structure at a higher hazard level (e.g., DBE, MCE) is larger than that at a lower hazard level (e.g., FOE). For this reason, ground motion suits with a reasonable number of records are required to reliably assess the seismic performance of a structure in terms of residual story drift response.

For the structures under the FOE, the EDPs are substantially reduced by incorporating the damping devices in the structure. In particular, the mean peak story drift and residual story drift response are reduced by up 70% and 90%, respectively, which essentially eliminated the permeant deformation of the structure and achieved the fully operational performance after the shaking of the earthquakes. According to the criteria in ASCE/SEI 41-06, the use of supplemental damping devices elevated the performance of the structure from "Life Safety" to "Immediate Occupancy" which requires a peak story drift ratio of less than 0.7%. In addition, the supplemental damping devices considerably reduced the peak floor velocity and peak floor acceleration EDPs that are more correlated with the damages of nonstructural components by nearly 50%. The mean peak floor acceleration response is diminished to 0.2 g, which indicates the nonstructural components in the building would be robust if designed following the requirement of Section 13.3 of ASCE/ SEI 7-10 that the horizontal design force of nonstructural components shall not be taken less than 30% of the component's seismic weight for a building site with $S_{DS} = 1.0$ g and nonstructural component importance factor $I_{\rm p}=1.0$.

For the structures under the DBE, the undamped structure has a mean peak story drift of 2.52%, thus barely achieved the "Life Safety" performance by meeting the story drift limitation requirement of 2.50% in ASCE/SEI 41–06 for the risk category I or II structures that represent a low risk to human life in the event of failure. The damped structure has significantly less story drift response than the undamped structure, and satisfies the drift limitation requirement of 1.50% in ASCE/SEI 41–06 for risk category IV structures (i.e., structures that are designated as essential facilities). In parallel, the supplemental damping devices validly reduced the residual story drift by 70% to only 0.11%. However, the reduction in the peak floor acceleration is not as effective as in the peak floor velocity under the DBE, neither as effective as that under the FOE

During the shaking of the MCE hazard level ground motions, the incorporation of the damping devices improved the seismic performance of the structure from the "Collapse Prevention" level with the peak story drift ratio of 4.29% to the "Life Safety" level with the peak story drift ratio of 2.33%. As well, the residual story drift of the undamped structure is reduced to a value of less than 0.5% which is considered as a limitation that can affect the function of nonstructural components such

Table 5Reduction of structural response under FOE hazard level ground motions.

Structure	re Peak story drift		Residual story drift		Floor velocity		Floor accele	ration	MRF base She	ar	Structure base shear	
	Mean (%)	CoV	Mean (%)	CoV	Mean (m/s)	CoV	Mean (g)	CoV	Mean (kN)	CoV	Mean (kN)	CoV
Undamped	1.31	0.18	0.11	0.89	0.49	0.14	0.38	0.11	491	0.08	729	0.10
Damped	0.39	0.22	0.01	0.35	0.20	0.17	0.21	0.15	233	0.22	507	0.16
Reduction	70%		92%		59%		45%		53%		30%	

Table 6Reduction of structural response under DBE hazard level ground motions.

Structure	ructure Peak story drift		Residual story drift		Floor velocity		Floor accele	ration	MRF base She	ar	Structure base shear	
	Mean (%)	CoV	Mean (%)	CoV	Mean (m/s)	CoV	Mean (g)	CoV	Mean (kN)	CoV	Mean (kN)	CoV
Undamped	2.52	0.23	0.37	0.98	0.80	0.14	0.57	0.12	637	0.06	1008	0.09
Damped	1.17	0.25	0.11	1.04	0.47	0.17	0.47	0.15	493	0.18	928	0.18
Reduction	54%		70%		41%		18%		23%		8%	

Table 7Reduction of structural response under MCE hazard level ground motions.

Structure	re Peak story drift		Residual stor	y drift	Floor velocity		Floor accele	ration	MRF base She	ear	Structure base shear	
	Mean (%)	CoV	Mean (%)	CoV	Mean (m/s)	CoV	Mean (g)	CoV	Mean (kN)	CoV	Mean (kN)	CoV
Undamped	4.29	0.23	1.05	0.82	1.13	0.15	0.70	0.12	714	0.07	1173	0.07
Damped	2.33	0.24	0.47	0.87	0.81	0.16	0.64	0.14	653	0.08	1278	0.12
Reduction	46%		55%		28%		9%		8%		-9%	

as doors, windows, and interior partitions [55–56]. Thus, the damped structure is essentially operational after an MCE earthquake event. The reductions in the peak floor velocity and peak floor acceleration under the MCE are much less than that under the FOE and DBE, which indicates the efficacy of the supplemental damping in mitigating the floor velocity and floor acceleration response declines with the increases of ground motion intensity. The reductions in the floor acceleration are highly correlated with the reductions in the MRF base shear. This observation validates that the efficacy of supplemental damping in floor acceleration suppression diminishes when the peak floor acceleration is related to the lateral strength of the structure after the yielding of the MRF at higher intensity levels of earthquakes.

Also can be observed is that, due to the inclusion of the damper force that is in-phase with the story drift of the supplemental damping system, the base shear of the damped structure does not necessarily decrease from that of the undamped structure. At the FOE hazard level, when the MRF of the damped structure is essentially elastic and has a much smaller story drift than the MRF of the undamped structure, the decrease of the base shear from the undamped structure to the damped structure is significant. At the DBE hazard level, with the occurrence of yielding in the MRF of the damped structure, the discrepancy in the base shear of the MRF between the damped and undamped structures diminishes, which reduces the discrepancy in the total base shear from the undamped structure to the damped structure. At the MCE hazard level, when the MRFs of both the damped and undamped structures are substantially yielded and have similar base shear forces, the inclusion of the damper force that is in-phase with the story drift of the structure under the perversely causes the total base shear increases from the undamped structure to the damped structure.

6.2. Probability distribution of EDPs

Fig. 7 shows the probability of exceedance (POE) of the peak story drift of the structures under the FOE, DBE, and MCE hazard level ground motions. In the figure, the data points are the POE by counting the sorted peak values of the EDPs from the dynamic analysis using the suite of 40 ground motions at each hazard level, and the continuous lines are the lognormal distribution that fits the data points. In order to verify whether a lognormal probability distribution can be assumed for the EDPs, a Kolmogorov-Smirnov goodness of fit test [57] is conducted. It can be seen that the lognormal probability distribution assumption is reasonable for the story drift response of both the undamped and damped structures. Accordingly, the probability of the peak story drift exceeding the limit for a certain performance level can be estimated. For instance, the failure probability for the "Life Safety" and "Collapse prevention" performance level for the undamped structure can be predicted as 47% and 21% under the DBE and MCE hazard level ground motions, respectively. And it is predictable that the damped structure can essentially eliminate the risk of structural failure causing life safety under the DBE and building collapse under the MCE. The lognormal probability distribution assumption is also applied to the peak floor velocity and peak absolute floor acceleration at all hazard levels. As shown in Fig. 8 and Fig. 9, though the fits of the data with the lognormal probability distribution for floor velocity and floor acceleration are not as good as that for story drift, still all data points lie between the limits of acceptability. Hence, the lognormal assumption is also reasonable for floor velocity and floor acceleration response. This is a very important observation since this provides a basis for the prediction of economic losses due to damages of nonstructural components.

Fig. 10 shows the variations of logarithmic standard deviations of the EDPs over earthquake intensity levels. It can be seen that, for both the undamped and damped structures, the logarithmic standard deviations

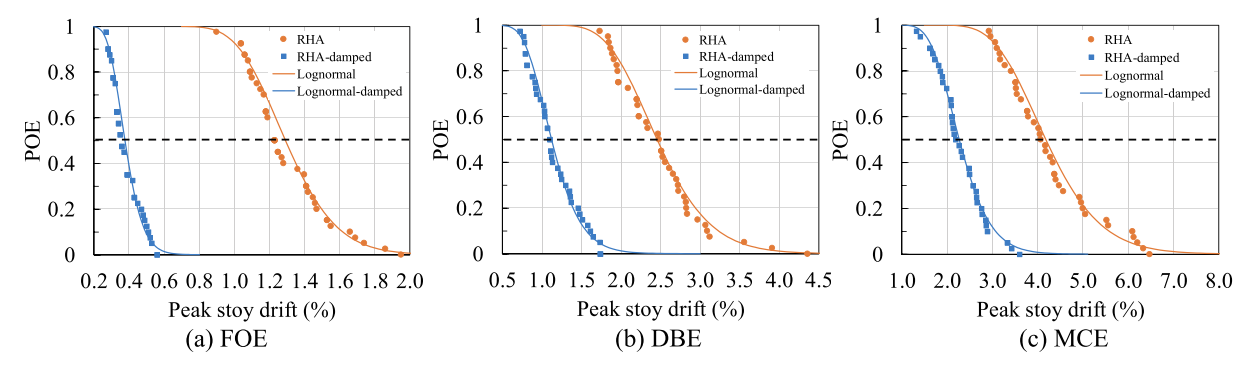


Fig. 7. Lognormal probability distribution of peak story drift response at various hazard levels of intensity.

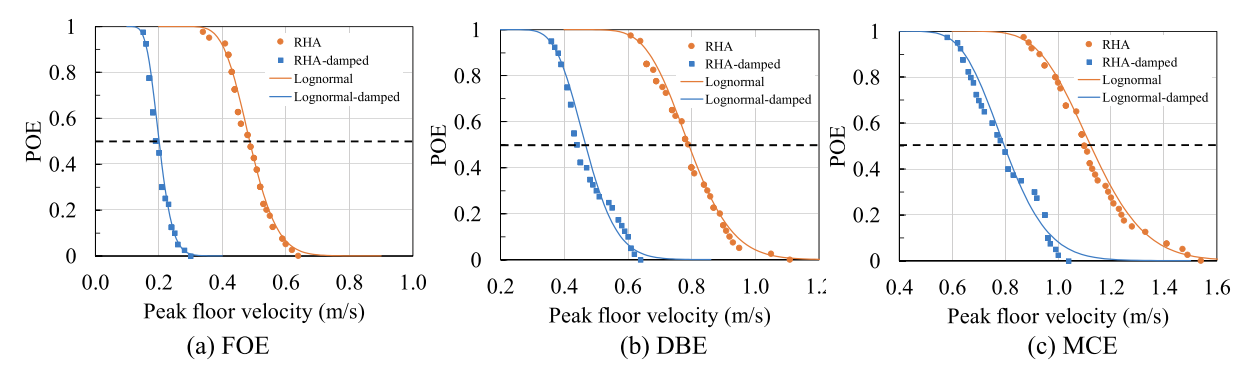


Fig. 8. Lognormal probability distribution of peak floor velocity response at various hazard levels of intensity.

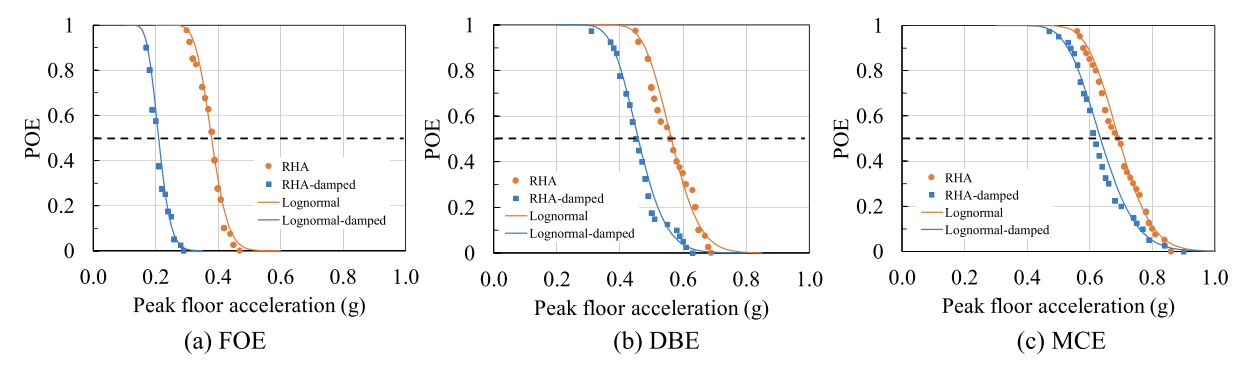


Fig. 9. Lognormal probability distribution of peak floor acceleration response at various hazard levels of intensity.

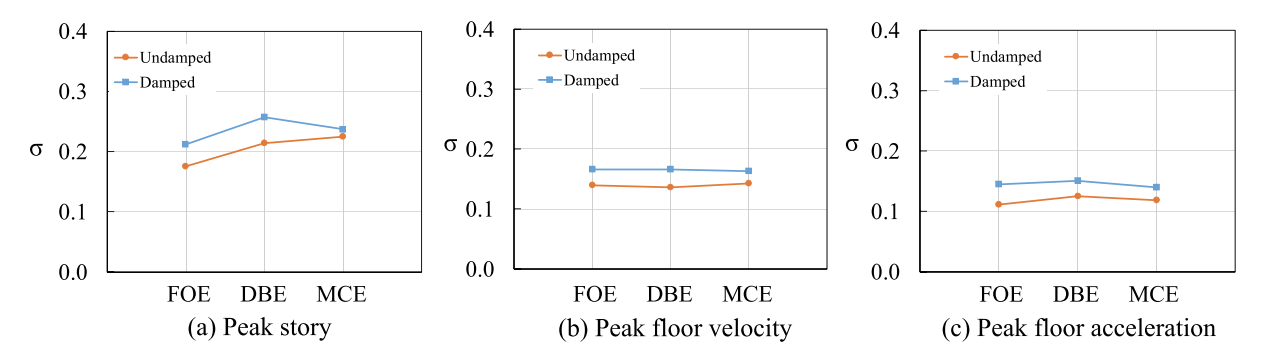


Fig. 10. Variations of logarithmic standard deviation of EDPs with earthquake intensity level.

 (σ) for the considered EDPs are small and do not obviously increase with the increasing of ground motion intensity. Particularly, the logarithmic standard deviations of peak floor velocity and peak floor acceleration are rather uniform at various levels of ground motion intensities, indicating that these EDPs have comparable shapes of a lognormal probability distribution. Moreover, the logarithmic standard deviations of these EDPs are approximately equivalent to the average lognormal standard deviations of the spectral accelerations of ground motions (which is 0.25 as given in Section 4), indicating the variability in the selected ground motions leads no increase of uncertainties in the considered EDPs for both the undamped and damped structures.

7. Summary and conclusions

A study is performed to implement the performance-based earthquake engineering (PBEE) framework to relate site-specific earthquake hazard to structural response prediction for structures with variable dynamic properties. Stated are the differences between the risk-target hazard from ASCE/SEI 7–10 seismic design maps and the site-specific hazard from probabilistic seismic hazard analysis (PSHA), as well as the suitability of ground motion selection approaches using the uniform hazard spectrum (UHS) and conditional mean spectrum (CMS) as the target hazard spectrum for structures with variable dynamic properties. Based on this, a site-specific ground motion selection procedure using the UHS is proposed for structures with supplemental damping devices. Then, three suites of 40 ground motions at hazard level intensities with 2%, 10%, and 50% probability of exceedance in 50 years, representing the FOE, DBE, and MCE seismic intensities, are selected for a paradigm building site. These ground motions are used for the dynamic analysis of a performance-based design prototype structure with nonlinear viscous dampers. Using the results from the dynamic analysis, evaluated are the probabilistic distributions of major engineering demand parameters (EDPs) including peak story drift, residual story drift, peak floor velocity, and peak floor acceleration, as well as the effectiveness of supplemental damping in structural resilience enhancement. The major conclusions of this study are as follows:

- (1) The UHS-based site-specific ground motion selection procedure is able to generate ground motion suites for reliable response quantification of structures with variable dynamic properties (e. g., structures with supplemental damping systems).
- (2) Using the UHS-based site-specific ground motion selection procedure, the major EDPs, including peak story drift, peak floor velocity, and peak floor acceleration response, can be estimated using a probabilistic approach.
- (3) By relating site-specific hazard to performance quantification, the UHS-based site-specific ground motion selection procedure is critical to the performance assessment of structures with variable dynamic properties in the PBEE framework.
- (4) With a better characterization of earthquake hazard and probability observation of structural response from dynamic analysis in the PBEE framework, the paradigm type of structure with supplemental nonlinear viscous dampers can be better used for structural resilience enhancement under various levels of seismic intensity.

Using the structure with supplemental viscous damping devices as a paradigm of structures with variable dynamic properties, this study demonstrates the estimations of EDPs using a site-specific UHS-based method of ground motion selection is critical to the structural performance assessment. Insights from this study can be utilized for future development of a more rigorous approach to assess the conditional probability distribution of the major EDPs on ground motion uncertainty for various types of structures (e.g., structures with semi-active or active structural control technology, self-centering technology, and base isolation technology, that are not considered as the context in the study) with a broad range of design parameters and building sites. Continuing on this work, the authors believe it would be meaningful to develop a database of structural response at various intensity levels of ground motions and a probabilistic model that can be used to reliably assess the conditional probability distribution of EDPs accounting for the uncertainty in ground motions. Using this database and model, the PBEE framework can be better implemented to quantify the risk of structures in future ground motions.

CRediT authorship contribution statement

Baiping Dong: Conceptualization, Methodology, Project administration, Funding acquisition, Investigation, Visualization, Data curation, Writing – original draft, Writing – review & editing. **James M. Ricles:** Methodology, Investigation, Writing – review & editing.

Declaration of Competing Interest

The authors declare that they have no known competing financial interests or personal relationships that could have appeared to influence the work reported in this paper.

Data availability

Data will be made available on request.

Acknowledgments

Gratefully acknowledged is the financial support by the National Natural Science Foundation of China (NSFC) (grant No. 52078385) and the Science and Technology Commission of Shanghai Municipality (Pujiang Program: 20PJ1414000). The support from Prof. Richard Sause at Lehigh University is greatly appreciated. Also, the authors would like to thank the anonymous reviewers for their many comments and suggestions that improved the paper.

References

- Bruneau M, Chang SE, Eguchi RT, Lee GC, O'Rourke TD, Reinhorn AM, et al. A framework to quantitatively assess and enhance the seismic resilience of communities. Earthg Spectra 2003;19(4):733–52.
- [2] Bruneau M, Reinhorn A. Exploring the concept of seismic resilience for acute care facilities. Earthq Spectra 2007;23(1):41–62. https://doi.org/10.1193/1.2431396.
- [3] UNISDR. Living with risk: a global review of disaster reduction initiatives, United Nations Pub 2004. http://www.unisdr.org/we/inform/publications/657.
- [4] NRC (National Research Council). National Earthquake Resilience: Research, Implementation, and Outreach. The National Academies Press, Washington, DC, 2011.
- [5] Cutter SL, Burton CG, Emrich CT. Disaster resilience indicators for benchmarking baseline conditions. J Homel Secur Emerg Manage 2010;7(1):Article 51.
- [6] Cutter SL. Building disaster resilience: steps toward sustainability. Challenges Sustain 2014;1(2):72–9.
- [7] Poland C. The Resilient City: defining what San Francisco needs from its seismic mitigation polices: 2019. http://www.spur.org/initiative/resilient-city.
- [8] Poland C. Guidelines for creating disaster-resilient communities. In: Proceedings of 15th world conference earthquake engineering, Lisbon; 2012.
- [9] Burton HV, Deierlein GG, Lallemant D, Lin T. Framework for incorporating probabilistic building performance in the assessment of community seismic resilience. J Struct Eng 2016;142(8).
- [10] Bruneau M, Reinhorn AM. Structural engineering dilemmas, resilient EPCOT, and Other Perspectives on the Road to Engineering Resilience. ASCE-ASME J. Risk Uncertain. Eng. Syst. Part A Civ Eng 2019;5(3).
- [11] FEMA. Next-Generation Performance-Based Seismic Design Guidelines Program Plan for New and Existing Buildings. FEMA-445, Washington, DC, 2006.
- [12] FEMA. Development of Next Generation Performance-Based Seismic Design Procedures for New and Existing Buildings. FEMA P-58, Washington, DC, 2018.
- [13] Cornell CA. Engineering seismic risk analysis. Bull Seismol Soc Am 1968;58(5): 1583-606
- [14] Baker JW, Bradley BA, Stafford PJ. Seismic Hazard and Risk Analysis. Cambridge, England: Cambridge University Press; 2021.
- [15] Deierlein GG, Reinhorn AM, Willford MR. Nonlinear structural analysis for seismic design. NEHRP Seismic design technical brief no 4, NIST GCR 10–917-5. Gaithersburg: NIST; 2010.
- [16] Ibarra L, Medina R, Krawinkler H. Hysteretic models that incorporate strength and stiffness deterioration. Earthq Eng Struct Dyn 2005;34:1489–511.
- [17] Ellingwood B. Earthquake risk assessment of building structures. Reliab Eng Syst Saf 2001;74(3):251–62.
- [18] Liel AB, Deierlein GG. Cost-benefit evaluation of seismic mitigation alternatives for older reinforced concrete frame buildings. Earthq Spectra 2013;29(4):13911411.
- [19] Shome N, Cornell CA, Bazzurro P, Carballo JE. Earthquakes, records, and nonlinear responses. Earthq Spectra 1998;14(3):469–500. https://doi.org/10.1193/ 1.1586011.
- [20] Baker JW, Cornell CA. A vector-valued ground motion intensity measure consisting of spectral acceleration and epsilon. Earthq Eng Struct Dyn 2005;34(10):1193–217.
- [21] Baker JW, Cornell CA. Spectral shape, epsilon and record selection. Earthq Eng Struct Dyn 2006;35(9):1077–95.
- [22] Baker JW. Conditional mean spectrum: tool for ground-motion selection. J Struct Eng 2011;137(3):322–31.
- [23] Bradley BA. A generalized conditional intensity measure approach and holistic ground motion selection. Earthq Eng Struct Dyn 2010;39:1321–42.
- [24] Haselton CB, Baker JW, Liel AB, Deierlein GD. Accounting for ground-motion spectral shape characteristics in structural collapse assessment through an adjustment for epsilon. J Struct Eng 2011;137(3).
- [25] Kadas K, Yakut A, Kazaz I. Spectral ground motion intensity based on capacity and period elongation. J Struct Eng 2011;137(3):401–9.
- [26] Jayaram N, Lin T, Baker JW. A computationally efficient ground-motion selection algorithm for matching a target response spectrum mean and variance. Earthq Spectra 2011;27(3):797–815.
- [27] PEER. Evaluation of Ground Motion Selection and Modification Methods: Predicting Median Interstory Drift Response of Buildings. PEER Report 2009/01. Pacific Earthquake Engineering Research Center, University of California, Berkeley, 2009.
- [28] NIST. Selecting and Scaling Earthquake Ground Motions for Performing Response History Analysis, NIST/GCR 11-917-15, prepared by the NEHRP Consultants Joint Venture for the National Institute of Standards and Technology, Gaithersburg, Maryland. 2011.
- [29] Constantinou MC, Symans MD. Experimental and analytical investigation of seismic response of structures with supplemental fluid viscous dampers. NCEER Rep. No. 92-0032. Buffalo, NY: State Univ. of New York; 1992.
- [30] Pekcan G, Mander JB, Chen SS. Fundamental considerations for the design of nonlinear viscous dampers. Earthq Eng Struct Dyn 1999;28(11):1405–25.
- [31] Christopoulos C, Filiatrault A. Principles of passive supplemental damping and seismic isolation. Pavia, Italy: IUSS Press; 2006.
- [32] Symans MD, Charney FA, Whittaker AS, Constantinou MC, Kircher CA, Johnson MW, et al. Energy dissipation systems for seismic applications: current practice and recent developments. J Struct Eng 2008;134(1):3–21.
- [33] Dong B, Sause R, Ricles JM. Seismic response and damage of reduced-strength steel MRF structures with nonlinear viscous dampers. J Struct Eng 2018;144(12): 04018221.
- [34] Almufti I, Willford M. Resilience-based earthquake design initiative (REDi) rating system for the next generation of buildings. Arup 2013.

- [35] Sause R, Hemingway GJ, Kasai K. Simplified seismic response analysis of viscoelastic-damped frame structures. In: Proc 5th US National Conf. on Earthquake Engineering I, Earthquake Engineering Research Institute (EERI), Oakland. CA: 1994.
- [36] Fu Y, Kasai K. Comparative study of frames using viscoelastic and viscous dampers. J Struct Eng 1998;124(5):513–22.
- [37] Lin W, Chopra A. Earthquake response of elastic single-degree-of-freedom systems with nonlinear viscoelastic dampers. J Eng Mech 2003;129(6):597–606.
- [38] Dong B, Sause R, Ricles JM. Seismic response and performance of a steel MRF building with nonlinear viscous dampers under DBE and MCE. J Struct Eng 2016; 142(6):04016023.
- [39] ASCE. Seismic Rehabilitation of Existing Buildings (ASCE/SEI 41-06). American Society of Civil Engineers, Reston, VA; 2007.
- [40] Building Seismic Safety Council (BSSC). NEHRP Recommended Seismic Provisions for New Buildings and Other Structures: FEMA P-750/2009 Edition. Federal Emergency Management Agency, Washington, DC; 2009.
- [41] ASCE. Minimum design loads for buildings and other structures, ASCE/SEI standard ASCE 7-10. ASCE, Reston; 2010.
- [42] Petersen MD et al. Documentation for the 2008 update of the United States national seismic hazard maps. US Department of the Interior, US Geological Survey; 2008. https://doi.org/10.3133/ofr20081128.
- [43] Campbell KW, Bozorgnia Y. NGA ground motion model for the geometric mean horizontal component of PGA, PGV, PGD and 5% damped linear elastic response spectra for periods ranging from 0.01 to 10 s. Earthq Spectra 2008;24(1):139–71.
- [44] Field EH, Jordan TH, Cornell CA. OpenSHA: A developing community-modeling environment for seismic hazard analysis. Seismol Res Lett 2003;74(4):406–19.
- [45] Boore DM, Atkinson GM. Ground-motion prediction equations for the average horizontal component of PGA, PGV, and 5%-damped PSA at spectral periods between 0.01 s and 10.0 s. Earthq Spectra 2008;24(1):99–138.

- [46] Chiou B-J, Youngs RR. An NGA model for the average horizontal component of peak ground motion and response spectra. Earthq Spectra 2008;24(1):173–215.
- [47] PEER NGA. Pacific Engineering Research Database; 2008. http://peer.berkeley. edu/nga.
- [48] Dong B, Ricles JM. Simplified seismic design procedure for steel MRF structure with nonlinear viscous dampers. J Constr Steel Res 2021. https://doi.org/10.1016/ i.icsr.2021.106857.
- [49] AISC. Specification for Structural Steel Buildings (ANSI/AISC 360-10). American Institute of Steel Construction, Chicago, Illinois, 2010.
- [50] AISC. Seismic Provisions for Structural Steel Buildings (ANSI/AISC 341-10). American Institute of Steel Construction, Chicago, Illinois, 2010.
- [51] OpenSees. Open System for Earthquake Engineering Simulation. Pacific Earthquake Engineering Research Center, University of California, Berkeley; 2012. Available at http://opensees.berkeley.edu/.
- [52] Dong B, Sause R, Ricles JM. Modeling of nonlinear viscous damper response for analysis and design of earthquake-resistant building structures. Bull Earthq Eng 2022;20:1841–64. https://doi.org/10.1007/s10518-021-01306-7.
- [53] Dong B. Large-scale experimental, numerical, and design studies of steel MRF structures with nonlinear viscous dampers under seismic loading. PhD Dissertation, Lehigh University; 2016.
- [54] Chopra AK. Dynamics of structures: theory and applications to earthquake engineering (4th Edition). New Jersey: Prentice Hall; 2011.
- [55] Galambos TV, Ellingwood B. Serviceability limit states: Deflection. J Struct Eng 1986;112(1):67–84.
- [56] McCormick J, Aburano H, Ikenaga M, Nakashima M. Permissible residual deformation levels for building structures considering both safety and human elements. In Proc., 14th World Conf. on Earthquake Engineering. Beijing: World Conference on Earthquake Engineering; 2008.
- [57] Benjamin J, Cornell CA. Probability, statistics, and decision for civil Engineers. New York: McGraw-Hill; 1970.